ANALYSIS OF TWO-SECTION RESONANT VOLTAGE CONVERTER FOR MATRIX LED LIGHT SOURCE DRIVERS

Anatolii Lupenko[1], Ivan Sysak[2], Michal Frivaldsky [3], Taras Chomko [4]

[1]Ternopil Ivan Puluj National Technical University, Ruska str. 56, 46001, Ternopil, Ukraine; lupenkoan@gmail.com
[2]Ternopil Ivan Puluj National Technical University, Ruska str. 56, 46001, Ternopil, Ukraine; sisak.tntu@gmail.com
[3]University of Zilina, Slovakia; michal.frivaldsky@feit.uniza.sk
[4]Ternopil Ivan Puluj National Technical University, Ruska str. 56, 46001, Ternopil, Ukraine; tarasvarikap@gmail.com

Abstract: Analysis of two-section resonant DC-to-DC converter with phase power control, which is the basis of the matrix LED light source driver is carried out. Two-section converter is considered as a boundary case of the multi-section converter with one controlled section and other uncontrolled sections. Analysis is carried out by the fundamental harmonic approximation method. Analytical expressions for complex voltages and currents in the converter sections are determined, its control characteristic is obtained. It is shown that the converter power can be controlled within the range from the maximum value to zero. The problems of operation of section transistor switches in their zero-voltage switching mode is considered. The verification of the proposed analysis by means of converter simulation is carried out. The simulation results are in good agreement with the analysis results.

Keywords: *two-section resonant inverter, power, phase control, zero-voltage switching.*

1. Introduction

Matrix LED light sources are becoming widespread in modern lighting systems, due to their high light output, the ability to create powerful lighting systems, long service life, small size, ease of implementation of lighting devices for both indoor and outdoor lighting [1]. They make it possible to build high-quality dimming energy-efficient lighting devices. Matrix LED is powered by drivers - power electronics devices that form a comfortable electromagnetic environment for both matrix LED and electrical network. The main stage in the chain of power conversion in such drivers is a DC-DC converter with controlled output voltage (current) to operate the matrix LED. Therefore, the investigation of approaches to the design of such DC-DC converters is of great interest to the scientists.

2. Analysis of the available investigations

A considerable part of investigations of DC-DC converter for LED drivers is devoted to DC-DC converters with pulse width modulation (PWM) control. The driver with Buck-Boost converter which simultaneously performs the function of power factor correction of the driver is considered in paper [2]. In papers [3, 4], a Buck converters which operate in a wide range of input voltages are considered as a LED drivers. In paper [5] a Flyback converter and in paper [6] a modified SEPIC-converter are considered as well. The main disadvantage of PWM converters is relatively low efficiency due to switching losses in power switches. Since the switching losses are proportional to the switching frequency, the operating frequencies of such converters are relatively low, which restrain the improvement of their mass and volume parameters.

In papers [7, 8] drivers of LED light sources with resonant DC-DC converters are considered. Such converters have a high efficiency due to low switching losses in power switches ("soft" switching) and better electromagnetic compatibility. Thus, in paper [7] the driver is implemented on the basis of a half-bridge resonant inverter, but such driver does not provide light source dimming, which limits its use by individual lamps. In the driver [8], a full-bridge resonant inverter with wide range power control by means of changing the phase shift between the rectangular pulses of the inverter arms is used as DC-DC converters. This driver is well suited for controlling of matrix LED in high-quality lighting systems, but its maximum power may be limited by the power of transistor switches and magnetic components. In order to remove this limitation, we can apply the approach proposed in paper [9], which consists in the parallel operation of N (N - number of sections) individual half-bridge resonant inverter sections on a common load. The maximum power of such inverter is proportional to the number N of its sections. The power control in such inverter is carried out by changing the phase shifts between rectangular pulses in individual sections.

In this paper, two-section (N=2) resonant DC-DC converter with phase power control is analyzed as a boundary case of multi-section resonant inverter [9]. A similar two-section converter is considered in paper [10], but in its analysis it is assumed that phase shifts of the resonant sections are mutually opposite and identical in modulus, which complicates the application of such analysis for multi-section converters, where phase shifts in inverter sections can be arbitrary (non-identical) and independent of each other. In multi-section DC-DC converter, only one section can be taken as reference (unregulated), relatively to which the phase shifts of other (regulated) sections are controlled. Then, by switching off the "redundant" sections of multi-section converter, it is possible to realise a step-continuous phase power control which provides less ouput LED power with a smaller number of sections, making it possible to increase the efficiency of the multi-section converter at medium and low power [11].

In this paper, such approach is proposed in the analysis of two-section DC-DC converter as a boundary case of multi-section DC-DC converter with phase control, for its further development in the analysis of multi-section resonant converter with arbitrary number of sections.

The objective of the paper is to investigate the parameters and characteristics of two-section resonant DC-DC converter, made on the basis of two half-bridge resonant inverter sections, while ensuring constant operating frequency.

Statement of the problem. Two-section resonant converter is shown in Fig.1. Each of its sections consists of half-bridge inverter on transistors *VT1, VT2* (*VT3, VT4*), the which outputs are connected to parallel resonant capacitor *C* by means of coupling capacitors C_s and inductors *L* and the primary winding of transformer *T*. Half-bridge voltages at nodes A_1 and A_2 are periodic rectangular pulses (Fig. 2), shifted by controlled angle $\varphi=0\div\pi$ rad. The amplitude of these pulses is equal to the supply voltage *E*, and their duty-cycle is close to 0.5. Almost sinusoidal alternating voltage of the resonant capacitor *C* is applied to the rectifier through the transformer *T* with transformer turns ratio *n*. The rectifier output voltage is supplied to the load *R* (LED matrix) through the filter $L_\phi C_\phi$.

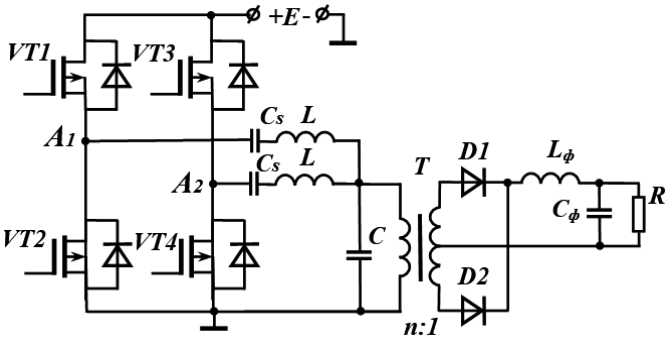

Fig. 1 Two-section resonant converter

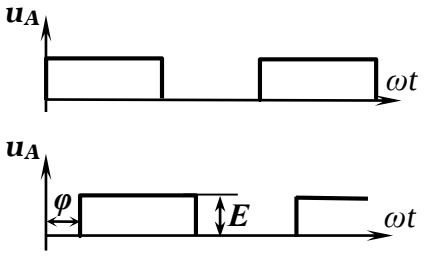

Fig. 2 Output voltages of half-bridge sections

Let us analyze the inverter by means of fundamental harmonic approximation, taking into account the filtering properties of the resonant circuits.

Statement of basic materials. The equivalent circuit of two-section inverter is shown in Fig. 3.

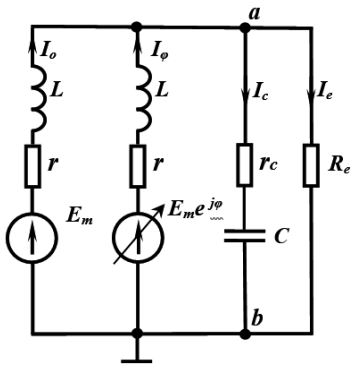

Fig. 3 Equivalent circuit of two-section inverter

In this circuit, the half-bridge square-wave sources are represented by fundamental harmonic voltage sources. The complex amplitudes of these voltage sources in reference and controlled sections are equal relatively to:

$$\underline{E}_m = \frac{2E}{\pi},\ \underline{E}_N = E_m e^{-j\varphi}. \tag{1}$$

The inverter effective load resistance R_e in Fig. 3 is the resistance of rectifier loaded by matrix LED reduced to the transformer primary winding. The effective resistance R_e of the center-tapped rectifier (Fig. 1) with ideal components is determined by the expression [12]:

$$R_e = \frac{\pi^2 n^2 R}{8}. \tag{2}$$

Switching and conductive losses in transistors and losses in inductors in each section may be taken into account by resistances *r*, and losses in the capacitor by resistance r_C (Fig. 3). These losses are considered to be significantly less than the power in the load, so these losses are neglected in order to simplify the analysis.

The parameters of the inverter and the relationship between them are shown in Table. 1: ω_0 is resonant frequency; ω is the inverter operating frequency; Z_0 is characteristic impedance of resonant tanks; Q is quality factor; Ω is relative operating frequency (the ratio of the inverter operating frequency ω to the resonant frequency ω_0).

Table 1

Inverter parameters and the relationship between them

$\omega_0 = \sqrt{\frac{2}{LC}}$	$Z_0 = \frac{2}{\omega_0 C}$
$R_e = \frac{QZ_0}{2}$	$Q = \frac{2R_e}{Z_0}$
$\omega C = \Omega \frac{2}{Z_0}$	$\omega L = \Omega Z_0$

The impedance at nodes *a*, *b* (Fig. 3) is equal to:

$$\underline{Z} = \frac{1}{j\omega C + \frac{1}{R_e}} = \frac{QZ_0}{2(1 + j\Omega Q)}. \tag{3}$$

The complex voltage amplitude at nodes *a, b* is represented by the following expression:

$$\underline{U}_{ab} = \frac{\sum_{i=1}^{2} \underline{E}_i \underline{g}_i}{\sum_{i=1}^{2} \underline{g}_i + \frac{1}{\underline{Z}}} = \frac{1}{2} \frac{E_m \frac{1}{j\Omega Z_0} + E_m e^{j\varphi} \frac{1}{j\Omega Z_0}}{\frac{1}{j\Omega Z_0} + \frac{1 + j\Omega Q}{QZ_0}} = \frac{E}{\pi} \frac{1 + \cos\varphi - j\sin\varphi}{\left(1 - \Omega^2\right) + j\frac{\Omega}{Q}}. \tag{4}$$

The maximum value of the inverter transfer function at the voltage of the first harmonic will be at the phase shift φ=*0*:

$$M_{1\max} = \frac{\left|U_{ab\max}\right|}{E_m} = \frac{1}{\sqrt{\left(1 - \Omega^2\right)^2 + \left(\frac{\Omega}{Q}\right)^2}}, \tag{5}$$

where $\left|U_{ab\max}\right|$ is the modulus of the maximum value of the complex voltage (4).

The quality factor of the resonant tank, which provides the maximum output voltage is equal to:

$$Q = \frac{M_{1\max}\Omega}{\sqrt{1 - M_{1\max}^2 \left(1 - \Omega^2\right)^2}}. \tag{6}$$

The phasor of current $\underline{I}_0$ of the reference section is equal to:

$$\underline{I}_0 = \frac{E_m - \underline{U}_{ab}}{j\Omega Z_0} = \frac{2E}{\pi Z_0} \frac{\left[-\Omega + \frac{1}{2\Omega}(1 - \cos\varphi)\right] + j\left[\frac{1}{2\Omega}\sin\varphi + \frac{1}{Q}\right]}{j\left(1 - \Omega^2\right) - \frac{\Omega}{Q}}. \tag{7}$$

The phasor of current of the inverter controlled section is described by the following expression:

$$\underline{I}_{\varphi} = \frac{E_m e^{-j\varphi} - \underline{U}_{ab}}{j\Omega Z_0} = \frac{2E}{\pi Z_0} \frac{\left[\left(\frac{1}{2\Omega} - \Omega\right)\cos\varphi + \frac{1}{Q}\sin\varphi - \frac{1}{2\Omega}\right] + j\left[\left(\Omega - \frac{1}{2\Omega}\right)\sin\varphi + \frac{1}{Q}\cos\varphi\right]}{j\left(1-\Omega^2\right) - \frac{\Omega}{Q}}. \quad (8)$$

The phasor of current I_c of the resonant capacitor is represented by the expression:

$$\underline{I}_c = j\frac{2\Omega}{Z_0}\underline{U}_{ab} = \frac{2E}{\pi Z_0}\Omega \frac{\sin\varphi + j(1+\cos\varphi)}{j\left(1-\Omega^2\right) - \frac{\Omega}{Q}}. \quad (9)$$

The phasor of inverter output current (in effective resistance R_e) is equal to:

$$\underline{I}_e = \frac{\underline{U}_{ab}}{R_e} = \frac{2E}{\pi Q Z_0} \frac{1+\cos\varphi - j\sin\varphi}{j\left(1-\Omega^2\right) - \frac{\Omega}{Q}}. \quad (10)$$

Using expressions (7 ÷ 10) the dependences of normalized amplitudes of the currents I_c, I_0, I_φ, I_e (reduced to factor $2E/\pi Z_0$) as a function of a phase shift are calculated and shown in Fig. 4. The inverter parameters are Ω=1.08 and Q=2.7.

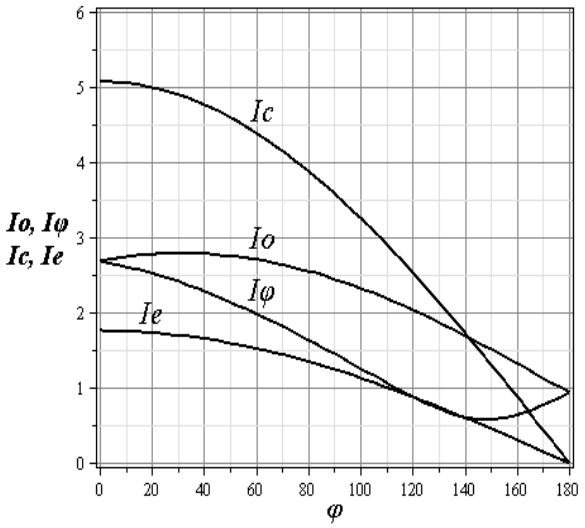

Fig. 4 Normalized amplitudes of the currents versus phase shift

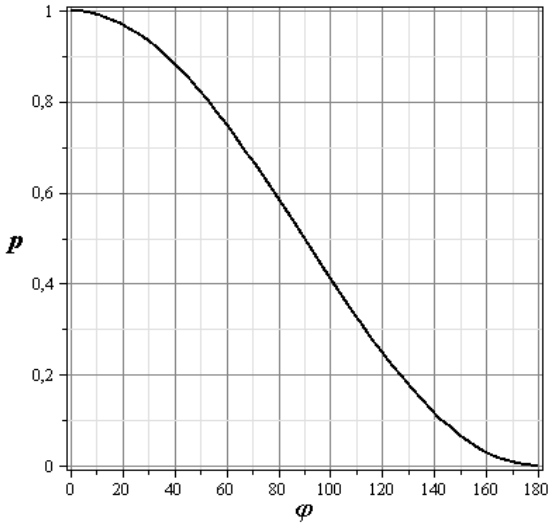

Fig. 5 Inverter normalized power versus phase shift

The inverter power is determined by the following expression:

$$P = \frac{\underline{U}_{ab}\underline{I}_e^*}{2} = \frac{2E^2}{\pi^2 Q Z_0} \frac{1+\cos\varphi}{\left(1-\Omega^2\right)^2 + \left(\frac{\Omega}{Q}\right)^2}. \quad (10)$$

Maximum power of the inverter (at φ=0) is as follows :

$$P_{\max} = \frac{2E^2}{\pi^2 Q Z_0} \frac{2}{\left(1-\Omega^2\right)^2 + \left(\frac{\Omega}{Q}\right)^2}. \quad (11)$$

The dependence of the inverter normalized power $p = P/P_{\max}$ on the phase shift is shown in Fig.5. The inverter power is regulated within the range from 100% to 0 when changing the phase shift whithin the range from 0 to 180º.

The complex power supplied by reference section is equal to:

$$\underline{S}_0 = \frac{1}{2} E_m \underline{I}_0^* = \frac{E^2}{\pi^2\ \Omega\ Z_0} \frac{\sin\varphi + 2\frac{\Omega}{Q} + j\left(1-\cos\varphi-2\Omega^2\right)}{\left(1-\Omega^2\pi\right) - j\frac{\Omega}{Q}}. \quad (12)$$

The phase shift between voltage and current in the reference section is equal to:

$$\varphi_0 = arctg\ \frac{\left(1-\Omega^2\right)\left(1-\cos\varphi-2\Omega^2\right)+\frac{\Omega}{Q}\left(\sin\varphi+2\frac{\Omega}{Q}\right)}{\left(1-\Omega^2\right)\left(\sin\varphi+2\frac{\Omega}{Q}\right)-\frac{\Omega}{Q}\left(1-\cos\varphi-2\Omega^2\right)}. \quad (13)$$

The complex power supplied by control section is equal to:

$$\underline{S}_\varphi = \frac{1}{2} E_m e^{j\varphi} \underline{I}_\varphi^* = \frac{E^2}{\pi^2\ \Omega\ Z_0} \frac{\left(1-\Omega^2\right)\left(\sin\varphi-2\frac{\Omega}{Q}\right)-j\frac{\Omega}{Q}\left(1-\cos\varphi-2\Omega^2\right)}{\left(1-\Omega^2\right)-j\frac{\Omega}{Q}}. \quad (14)$$

The phase shift φ_φ between voltage and current in the control section is equal to:

$$\varphi_\varphi = arctg\ \frac{\left(1-\Omega^2\right)\left(1-\cos\varphi-2\Omega^2\right)+\frac{\Omega}{Q}\left(2\frac{\Omega}{Q}-\sin\varphi\right)}{-\frac{\Omega}{Q}\left(1-\cos\varphi-2\Omega^2\right)+\left(1-\Omega^2\right)2\frac{\Omega}{Q}-\sin\varphi}. \quad (15)$$

According to expressions (13), (15) the dependences of the phase shift φ_0 and the phase shift φ_φ between voltages and currents relatively in the reference (Fig. 6) and controlled (Fig. 7) sections on the phase shift φ between the sections at quality values Q=1, Q=3, Q=5 are shown. These dependences correspond to the results obtained in paper [10]. As a result of the computational experiment, it is determined that at frequency values Ω<1.08, the phase shift φ_φ in the controlled section becomes negative at some interval of phase shift φ_φ. Therefore inverter turns into capacitive operating mode and transistor zero-voltage switching becomes lost. Thus, in the case of two-section converter, the switching frequency should not exceed this value.

The efficiency value η is determined by the following expression:

$$\eta_i = \frac{1}{1+\frac{r\left(I_o^2+I_\varphi^2\right)}{I_e^2 R_e}}. \quad (16)$$

where I_0, I_φ are the amplitude (or current) values of the inverter currents .

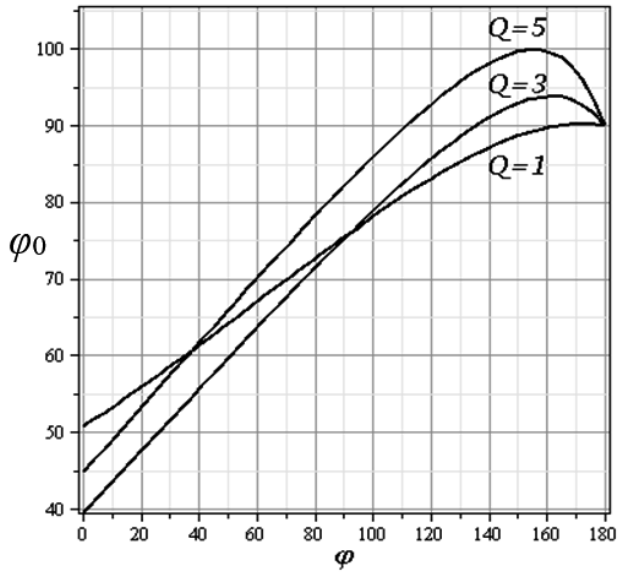

Fig. 6. Dependences of the phase shift φ_0 between voltage and current in the reference section on the phase shift φ between the sections for the quality factor values Q=1, Q=3, Q=5

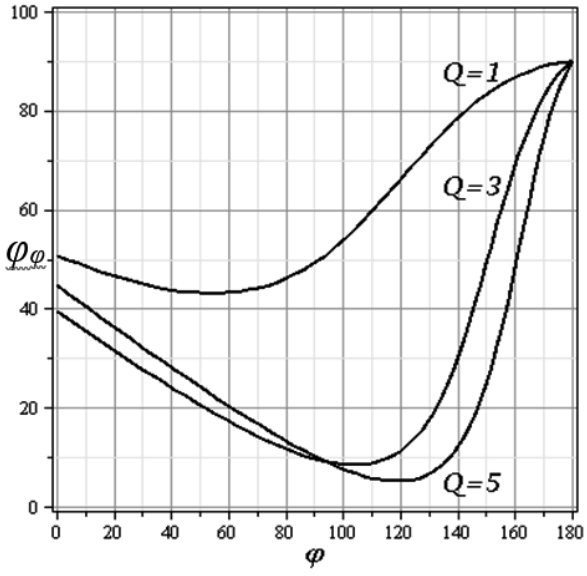

Fig. 7. Dependences of the phase shift φ_φ between voltage and current in the controlled section on the phase shift φ between the sections for quality values Q=1, Q=3, Q=5

Based on the carried out analysis, the parameters of the driver with two-section resonant voltage converter for power supply of EPSX-VF88 LED matrix are calculated. The matrix has nominal voltage 26 V and current 2.3 A. The converter is implemented on IRF730 transistors and MBR10100 diodes. The converter input voltage is E=110 V; the transformer turns ratio is n=4; operating frequency is f=110 kHz; inductance is L=239 μH; the capacity of the resonant capacitor is C=17.5 nF.

Simulation of the converter is carried out by means of the circuit simulator MicroCap-10. The simulation model is presented in Fig.8. In this model, the LED matrix EPSX-VF88 is replaced by resistor R=11.6 Ω. In order to take into account the losses in the inductors, 0.5 Ω resistors are connected with them in series.

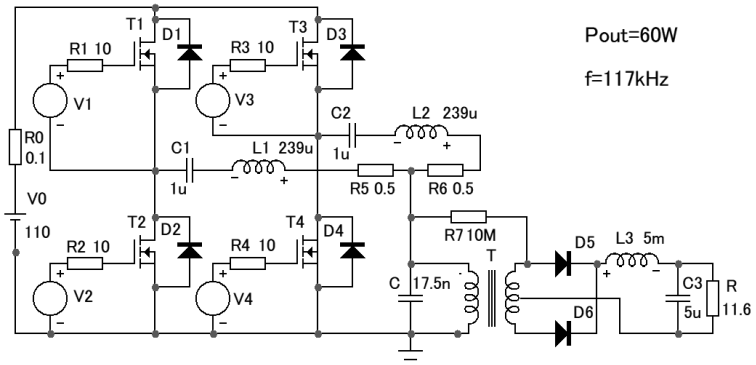

Fig. 8 The simulation model

The simulation results are presented in Fig. 9, that is: the upper oscillogram is voltage on the resonant capacitor (amplitude is 156 V); the middle oscillogram is voltage (26 V) on the LED matrix; the lower oscillogram is converter efficiency (0.96). The simulation results are in good agreement with the results of the analysis.

The carried out analysis can be extended to multi-section resonant inverters with continuous phase power control in one regulated section and step control by switching off the redundant sections when the inverter operates at medium and low power. Further research is required for the rational choice of the inverter operating frequency, at which the transistors zero-voltage switching is ensured in the entire converter power range.

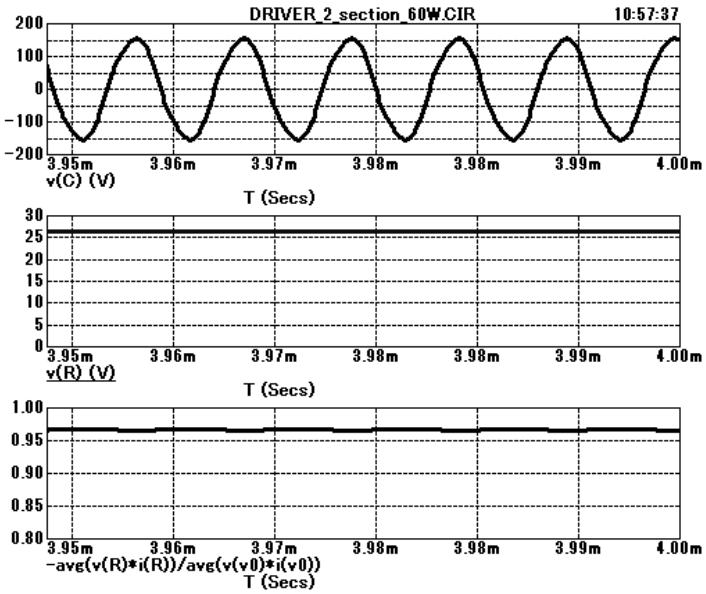

Fig. 9 Simulation results

3. Conclusions

The maximum inverter output power occurs during in-phase work of inverter sections. The inverter provides a wide range of power control in the load from the maximum value to zero when changing the phase shift between resonant sections from 0 to 180º. At the same time, the change of the phase shift between the sections causes the change of the phase shift between voltages and currents in its sections, which can turn the inverter into capacitive operating mode. Therefore, to ensure zero voltage switching of transistors in the whole power range, it is necessary while designing the inverter to select the inverter operating frequency in such a way that the phase shifts between voltages and currents are greater than zero by performing the computational experiment. The carried out analysis can be extended to multi-section resonant inverters with continuous phase power control with one controlled section and step control by switching off the redundant sections when the inverter operates at medium and low power.

References

1. Antypyn, S., Korolev, H. (2011). Svetodyodnuye matrytsu protyv odynochnukh svetodyodov. *Poluprovodnykovaia svetotekhnyka*, 5, 52-54.

2. Xu, R., Li, Y., Zhong, L., Liu, J. (2014). Research of an Efficient LED Lighting Driver Based on Boost-Buck Converter. *Circuits and Systems*, 5, 153-159.

3. Hamza, S., Mustafa, A. (2014). The use of Pulse Width Modulation "PWM" Technique in LED Lighting Systems. *International Journal of Science and Research*, *3*(11), 2316-2320.

4. Hu, Y., Huber, L., Jovanovic, M. (2012). Single-Stage, Universal-Input AC/DC LED Driver With Current-Controlled Variable PFC Boost Inductor. *IEEE Transactions on Power Electronics*, *27*(3), 1579-1588.

5. Lavanya, M., Tamilmani, S. (2017). Design and Analysis of Modified SEPIC Converter for LED Lamp Driver Applications. *International Journal of Advanced Research in Electrical, Electronics and Instrumentation Engineering*, *6*(3), 1627-1636.

6. Shrivastava, A., Singh, B. (2012). LLC Series Resonant Converter Based LED Lamp Driver with ZVS, *2012 IEEE Fifth Power India Conference*, Proceedings of International Conference, Murthal.

7. Jagadeesh, R. Vishwanathan, N. Porpandiselvi, S. (2018). An Efficient Parallel Resonant Converter for LED Lighting, *National Power Systems Conference*, Proceedings of the Conference, Tamilnadu.

8. Branas, C., Azcondo, F.J., Casanueva, R. (2008). A generalized study of multiphase parallel resonant inverters for high-power applications", *IEEE Transactions on Circuits and Systems I: Regular Papers, 55*(7), 2128-2138.

9. Kazimierczuk, M.K. (1993). Phase-controlled series-parallel resonant converter. *IEEE Transactions on Power Electronics*, *8*(3), 309 – 319.

10. Lupenko, A. (2020). Step-continuous phase power control of multi-section resonant inverter. *Computational problems of electrical engineering*, *10*(2), 7-12.

11. Kazimierczuk, M.K., Czarkowski, D. (2011). *Resonant power converters, 2nd Edition*. John Wiley & Sons.